

## Letters

### Silver Nanocoral Structures on Electrodes: A Suitable Platform for Protein-Based Bioelectronic Devices

Jiu-Ju Feng,<sup>†</sup> Peter Hildebrandt,<sup>†</sup> and Daniel H. Murgida<sup>\*‡</sup>

*Institut für Chemie, Technische Universität Berlin, Str. des 17. Juni 135, Sekr. PC14, D10623-Berlin, Germany, and Departamento de Química Inorgánica, Analítica y Química Física/INQUIMAE-CONICET, Facultad de Ciencias Exactas y Naturales, Universidad de Buenos Aires, Ciudad Universitaria, Pab. 2, piso 1, C1428EHA Buenos Aires, Argentina*

Received October 5, 2007. In Final Form: January 3, 2008

We report a simple strategy for constructing silver coral-like nanostructures on graphite electrodes suitable for bioelectronic applications. The nanocorals are conductive, have dimensions adequate for high protein loading, and are remarkably stable. They also provide a strong Raman surface enhancement that allows for in situ structural characterization of the immobilized proteins. The potential of the Ag nanocoral electrodes is exemplified by the construction and characterization of a hydrogen peroxide amperometric sensor based on cytochrome *c*.

The unique properties of proteins and enzymes in terms of redox behavior, molecular recognition, and catalysis represent an important potential for the design of bioelectronic devices, including biosensors, enzymatic reactors, and biofuel cells.<sup>1–4</sup> The assembly of such devices requires immobilization of the target proteins on electrodes under conditions that ensure the preservation of the native structures, efficient electronic communication, and a high protein load.

To that end, different experimental approaches have been employed ranging from the adsorption of proteins on electrodes coated with organic films to more complex structures including conductive polyelectrolytes, nanostructured materials and mesoporous films.<sup>5–22</sup>

Here we report a simple method for growing coral-like silver nanostructures on electrodes as a suitable platform for constructing protein-based bioelectronic devices.

Nanocoral structures were grown by electrodepositing Ag onto graphite substrates from a 5 mM AgNO<sub>3</sub>/0.1 M KNO<sub>3</sub> solution

\* Corresponding author. E-mail: dhmurgida@qi.fcen.uba.ar. Fax: +54 (11) 4576-3341.

<sup>†</sup> Technische Universität Berlin.

<sup>‡</sup> Universidad de Buenos Aires.

(1) Bullen, R. A.; Arnot, T. C.; Lakeman, J. B.; Walsh, F. C. *Biosens. Bioelectron.* **2006**, *21*, 2015–2045.

(2) Kim, J.; Jia, H. F.; Wang, P. *Biotechnol. Adv.* **2006**, *24*, 296–308.

(3) Newman, J. D.; Setford, S. J. *Mol. Biotechnol.* **2006**, *32*, 249–268.

(4) Willner, I.; Katz, E. *Angew. Chem., Int. Ed.* **2000**, *39*, 1180–1218.

(5) Jin, W.; Brennan, J. D. *Anal. Chim. Acta* **2002**, *461*, 1–36.

(6) Gerard, M.; Chaubey, A.; Malhotra, B. D. *Biosens. Bioelectron.* **2002**, *17*, 345–359.

(7) Chaubey, A.; Malhotra, B. D. *Biosens. Bioelectron.* **2002**, *17*, 441–456.

(8) Wang, J. *Electroanal.* **2001**, *13*, 983–988.

(9) Willner, I.; Katz, E.; Willner, B. *Electroanal.* **1997**, *9*, 965–977.

(10) Krajewska, B. *Enzyme Microb. Technol.* **2004**, *35*, 126–139.

(11) Gilardi, G.; Fantuzzi, A. *Trends Biotechnol.* **2001**, *19*, 468–476.

(12) Albareda-Sirvent, M.; Merkoci, A.; Alegret, S. *Sens. Actuators, B* **2000**, *69*, 153–163.

(13) Katz, E.; Willner, I. *ChemPhysChem* **2004**, *5*, 1085–1104.

(14) Murphy, L. *Curr. Opin. Chem. Biol.* **2006**, *10*, 177–184.

(15) Davis, F.; Higson, S. P. J. *Biosens. Bioelectron.* **2005**, *21*, 1–20.

(16) Bistolas, N.; Wollenberger, U.; Jung, C.; Scheller, F. W. *Biosens. Bioelectron.* **2005**, *20*, 2408–2423.

(17) Campas, M.; O'Sullivan, C. *Anal. Lett.* **2003**, *36*, 2551–2569.

(18) Willner, B.; Katz, E.; Willner, I. *Curr. Opin. Biotechnol.* **2006**, *17*, 589–596.

(19) Lin, Y. H.; Yantasee, W.; Wang, J. *Front. Biosci.* **2005**, *10*, 492–505.

(20) Wang, J. *Analyst* **2005**, *130*, 421–426.

(21) Katz, E.; Willner, I. *Angew. Chem., Int. Ed.* **2004**, *43*, 6042–6108.

(22) Beissenhirtz, M. K.; Scheller, F. W.; Stocklein, W. F. M.; Kurth, D. G.; Mohwald, H.; Lisdat, F. *Angew. Chem., Int. Ed.* **2004**, *43*, 4357–4360.

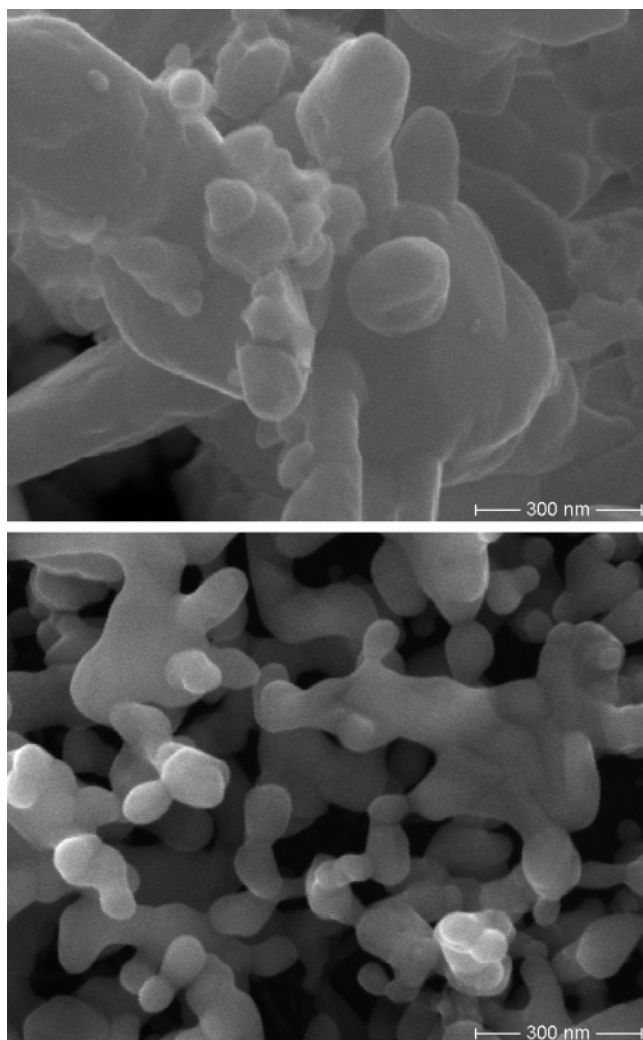


**Figure 1.** SEM images of Ag electrodeposited onto a graphite plate at  $-0.5$  V from an electrolyte solution containing  $5$  mM  $\text{AgNO}_3$  +  $0.1$  M  $\text{KNO}_3$  in the absence (top) and in the presence of  $0.1$  wt % SDS (bottom).

in the presence of  $0.1$  wt % sodium dodecyl sulfate (SDS) for  $4$  min at  $-0.5$  V. (All potentials cited in this work refer to the Ag/AgCl 3 M KCl electrode.) The surfactant was then removed by thoroughly washing with ethanol and water. The morphologies of the Ag films deposited in the absence and in the presence of SDS are compared in Figure 1. The adsorption of surfactants on electrodes has been reported to affect electron-transfer kinetics and, therefore, the structure of electrodeposits.<sup>23</sup> In the present case, SDS directs crystal growth favoring the formation of coral-like structures.

EDX analysis at several spots of the nanocoral films shows only a carbon peak at  $0.25$  eV from the graphite electrode used as a substrate for electrodeposition and Ag signals at  $3.1$  eV. The X-ray diffraction peaks are identified as Ag(111), (200), (220), and (311). The nanostructured electrodes were coated with a self-assembled monolayer (SAM) of mercaptohexanoic acid (MHA) by overnight incubation in a  $1$  mM MHA ethanol solution. After being thoroughly washed with ethanol and deionized water, the coated electrodes were incubated in a  $0.4$   $\mu\text{M}$  cytochrome *c* (Cyt) solution ( $10$  mM PBS, pH 7.0) for  $40$  min and rinsed with fresh buffer. The entire process was monitored by electrochemical impedance spectroscopy (EIS; Figure 2).

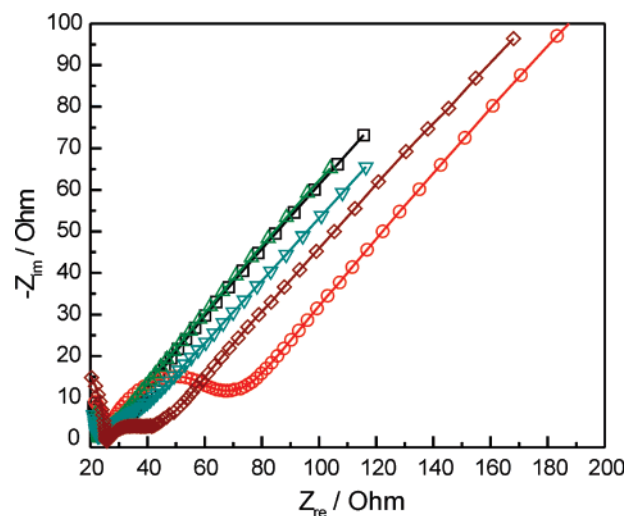


**Figure 2.** Electrochemical impedance spectra recorded at different stages of graphite electrode modification. Black squares: bare graphite. Red circles: Ag nanocoral with SDS. Green triangles: Ag nanocoral after the removal of SDS. Blue triangles: Ag nanocoral coated with an MHA-SAM. Maroon diamonds: SAM-coated Ag nanocoral after the adsorption of Cyt. Measurements were performed in  $0.10$  M KCl with  $5.0$  mM  $\text{K}_3\text{Fe}(\text{CN})_6/\text{K}_4\text{Fe}(\text{CN})_6$  ( $1:1$ ) using an alternating current voltage of  $5$  mV within the frequency range of  $10^{-2}$ – $10^5$  Hz.

Nyquist plots display the typical features for a cell in which polarization is due to a combination of charge transfer and diffusion processes (i.e., a semicircle and a linear part, respectively). The electrodeposition of nanocoral Ag on graphite electrodes in the presence of SDS results in a drastic increase in the electron-transfer resistance ( $R_{\text{et}}$ ), as indicated by a larger diameter of the semicircle in the Nyquist plot, which is ascribed to the adsorption of the surfactant. The effect is reversed upon SDS removal, indicating the good conductivity of the SDS-free nanocoral structures. SAM coating of the Ag films produces the expected increase in  $R_{\text{et}}$  because it reduces the accessibility of the redox probe to the surface. The effect becomes even more pronounced upon protein adsorption.

The integrity of the electrostatically immobilized protein was investigated by potential-dependent surface-enhanced resonance Raman (SERR) spectroscopy with excitation in resonance with the Soret transition of the heme. Under these conditions, SERR spectra are dominated by the totally symmetric modes of the porphyrin. The so-called marker band region (ca.  $1300$ – $1700$   $\text{cm}^{-1}$ ) includes a number of bands that are particularly sensitive to the electronic and structural properties of the heme, such as the ligation pattern, spin, and oxidation state.<sup>24–26</sup> SERR spectra of Cyt adsorbed on the SAM-coated nanocoral structures recorded at potentials sufficiently negative or positive with respect to the formal redox potential are identical to the resonance Raman spectra of ferrous and ferric Cyt in solution, respectively (Figure 3).

Thus, it is concluded that the immobilized protein retains the native structure, particularly at the level of the active site. Furthermore, the series of spectra recorded at intermediate potentials could be consistently simulated by the superposition of the component spectra of only the native ferric and ferrous Cyt just by varying their relative contributions. Quantitative

(23) Gomes, A.; Pereira, M. I. D. *Electrochim. Acta* **2006**, *52*, 863–871.

(24) Hu, S. Z.; Morris, I. K.; Singh, J. P.; Smith, K. M.; Spiro, T. G. *J. Am. Chem. Soc.* **1993**, *115*, 12446–12458.

(25) Murgida, D. H.; Hildebrandt, P. *Acc. Chem. Res.* **2004**, *37*, 854–861.

(26) Murgida, D. H.; Hildebrandt, P. *Top. Appl. Phys.* **2006**, *103*, 313–334.

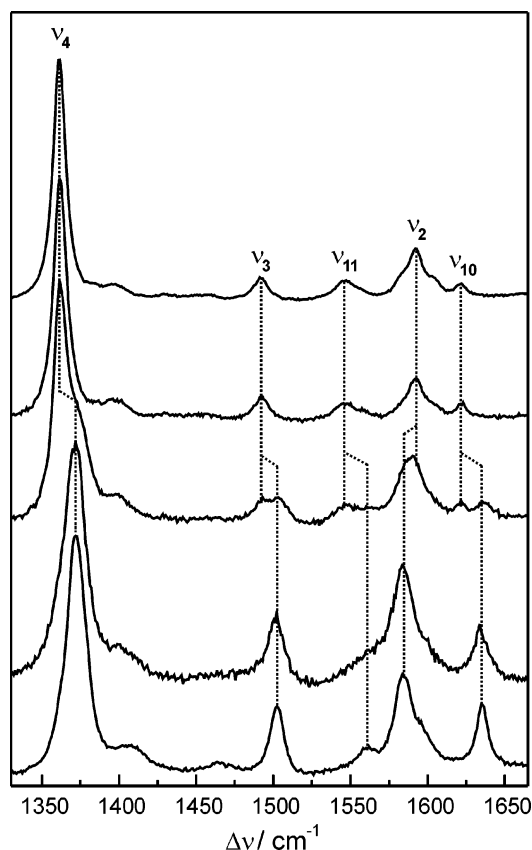


**Figure 3.** RR and SERR spectra of Cyt in solution and adsorbed onto SAM-coated Ag nanocoral electrodes, respectively. Top to bottom: RR of ferrous Cyt; SERR at  $-400$  mV; SERR at  $0$  V; SERR at  $150$  mV; and RR of ferric Cyt. Measurements were performed with  $413$  nm excitation. Marker bands are labeled according to ref 24.

treatment of the SERR spectra indicates that ca. 85% of the adsorbed protein is electrochemically active, and no spectral indication of denatured species was found. In contrast, Cyt directly adsorbed onto the bare Ag surfaces (i.e., without a SAM coating) shows the typical spectral features of non-native species, in agreement with previous observations.<sup>25</sup> Direct electron transfer of Cyt immobilized on SAM-coated nanocoral structures was further confirmed by cyclic voltammetry (Figure 4).

The average formal redox potential from several preparations was  $41 \pm 2$  mV, which is very close to the value for native Cyt in solution.<sup>27</sup> The full widths at half-height of the anodic and cathodic waves were ca.  $96 \pm 8$  mV, and the peak currents showed linear responses to the scan rate to the power of 0.75. This observation suggests that electron transfer is coupled to a non-Faradaic event, which most likely refers to the reorientation of the adsorbed protein.<sup>28,29</sup> In line with this interpretation, the apparent electron-transfer rate constant estimated from the peak separation as a function of the scan rate is ca.  $10$  s<sup>-1</sup> (Supporting Information). This value is clearly incompatible with a reaction mechanism in which electron tunneling is the rate-limiting event. Remarkably, peak currents are extremely stable, indicating that protein leaking is negligible. Indeed, almost no variations were observed after several scans in both directions using scan rates from  $10$  to  $500$  mV s<sup>-1</sup>. From the integration of the voltammetric

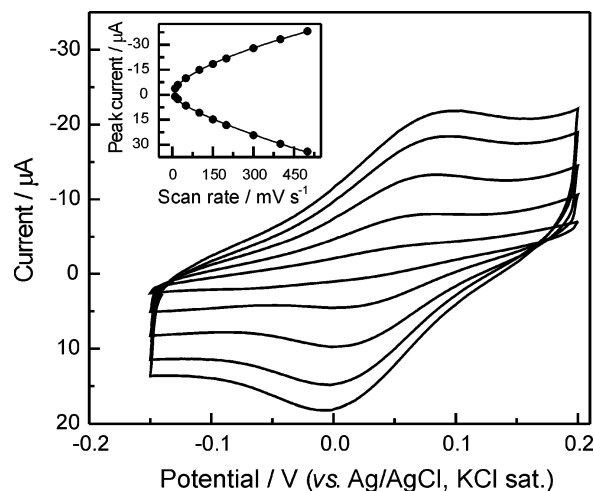


**Figure 4.** Cyclic voltammograms of Cyt adsorbed on SAM-coated Ag nanocoral electrodes recorded at different scan rates ( $10$ ,  $50$ ,  $100$ ,  $150$ , and  $200$  mV s<sup>-1</sup>) in  $10$  mM PBS buffer at pH  $7.0$ . Inset: peak currents as a function of the scan rate.

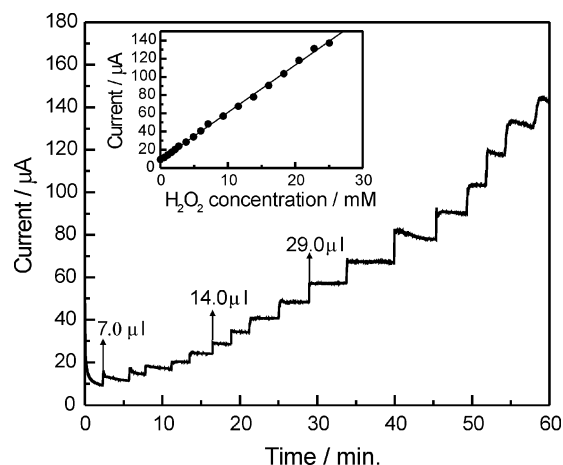


**Figure 5.** Amperometric responses of graphite/nanocoral/SAM/Cyt electrodes at  $-100$  mV upon successive additions of different volumes of  $5$  mM  $\text{H}_2\text{O}_2$  to the electrochemical cell containing  $5$  mL of  $10$  mM PBS buffer at pH  $7.0$ . Inset: linear response of the electrocatalytic current with  $\text{H}_2\text{O}_2$  concentration.

peaks and by considering the geometric area of the flat graphite substrate only, the surface concentration of Cyt is estimated to be  $\Gamma = 500$  pmol cm<sup>-2</sup>, which would correspond to ca. 50 fully packed protein monolayers. Given that under the present conditions Cyt can adsorb only to the SAM-coated Ag at submonolayer levels,<sup>25</sup> the number 50 represents the lower limit for the increase in the electroactive surface that is achieved upon Ag electrodeposition.

The hybrid electrodes were tested as hydrogen peroxide amperometric sensors. Current–time responses were recorded at  $-100$  mV after successive additions of  $\text{H}_2\text{O}_2$  with continuous stirring of the solution (Figure 5).

The catalytic currents respond linearly to the concentration of  $\text{H}_2\text{O}_2$  up to ca.  $23$  mM, after which a Michaelis–Menten-like plateau is reached. Thus, the detection range of the present devices is broader than those obtained for Cyt immobilized in NaY zeolite,<sup>30</sup> colloidal gold-modified carbon paste electrodes,<sup>31</sup> or

(27) Scott, R. A.; Mauk, A. G., Eds.; *Cytochrome C: A Multidisciplinary Approach*; University Science Books: Sausalito, CA, 1995.

(28) Murgida, D. H.; Hildebrandt, P. *Phys. Chem. Chem. Phys.* **2005**, *7*, 3773–3784.

(29) Avila, A.; Gregory, B. W.; Niki, K.; Cotton, T. M. *J. Phys. Chem. B* **2000**, *104*, 2759–2766.

(30) Dai, Z. H.; Liu, S. Q.; Ju, H. X. *Electrochim. Acta* **2004**, *49*, 2139–2144.

(31) Ju, H. X.; Liu, S. Q.; Ge, B. X.; Lisdar, F.; Scheller, F. W. *Electroanalysis* **2002**, *14*, 141–147.

(32) Wang, J.; Li, M.; Shi, Z.; Li, N.; Gu, Z. *Anal. Chem.* **2002**, *74*, 1993–1997.

carbon nanotube-modified electrodes.<sup>32,33</sup> Background catalytic currents measured on graphite/nanocoral/SAM electrodes were significantly lower and nonlinear (Supporting Information). The detection limit determined at a signal-to-noise ratio of 3 is 1.8  $\mu\text{M}$ , and the time to reach 90% of the maximum current after the addition of  $\text{H}_2\text{O}_2$  was less than 10 s in each case (i.e., faster than the one found for Cyt immobilized on a 3-mercaptopropionic acid monolayer-modified Au electrode<sup>34</sup>). Thus, the performance of the devices is comparable to that of more complex sensors based on Cyt or even on the intrinsically more efficient peroxidase enzyme.<sup>35–40</sup> Electrodes could be reused several times with reproducible responses. For example, five successive assays with the same electrode showed a dispersion of 3.4% for a given  $\text{H}_2\text{O}_2$  concentration (Supporting Information). Long-term stability is also within acceptable values. After a storage period of 2 weeks in buffer (10 mM PBS, pH 7.0) at 4 °C, the amperometric responses were found to be more than 95% of their initial values.

(33) Zhao, G. C.; Yin, Z. Z.; Zhang, L.; Wei, X. W. *Electrochem. Commun.* **2005**, *7*, 256–260.

(34) Gobi, K. V.; Mizunati, F. *J. Electroanal. Chem.* **2000**, *484*, 172–181.

(35) Poulsen, A. K.; Scharff-Poulsen, A. M.; Olsen, L. F. *Anal. Biochem.* **2007**, *366*, 29–36.

(36) Wang, F. C.; Yuan, R.; Chai, Y. Q. *Eur. Food Res. Technol.* **2007**, *225*, 95–104.

(37) Cao, S. R.; Yuan, R.; Chai, Y. Q.; Zhang, L. Y.; Li, X. L.; Gao, F. X. *Bioprocess Biosyst. Eng.* **2007**, *30*, 71–78.

(38) Yabuki, S.; Mizutani, F.; Hirata, Y. *J. Electroanal. Chem.* **1999**, *468*, 117–120.

(39) Lötzbeyer, T.; Schuhmann, W.; Schmidt, H. L. *Bioelectrochem. Bioenerg.* **1997**, *42*, 1–6.

(40) Moore, A. N. J.; Katz, E.; Willner, I. *J. Electroanal. Chem.* **1996**, *417*, 189–192.

The reproducibility of fabrication is better than 95%, as judged from the amperometric responses of three independent electrode preparations.

In conclusion, we have developed a very simple and inexpensive method for growing coral-like Ag nanostructures on graphite in a highly reproducible manner. The method has also been proven to be successful for ITO and gold substrates (not shown). The formation of the nanocoral structures is directed by the SDS surfactant. The modified electrodes show a good conductivity and can be easily coated with different alkanethiols for the subsequent biocompatible immobilization of biomolecules. As shown here for the case of Cyt, nanocoral structures constitute a powerful platform for the construction of protein-based bioelectronic devices in which a high, stable protein load is essential. Silver nanocorals offer the additional advantage of providing a strong Raman surface enhancement that allows for the in-situ structural characterization of the loaded protein as a prerequisite for the rational improvement of the devices.

**Acknowledgment.** Financial support by the Deutsche Forschungsgemeinschaft (Sfb 498-A8 and Cluster of Excellence “Unifying Concepts in Catalysis”), the Volkswagen Stiftung (I/80816) and ANPCyT (PICT2006-459) is gratefully acknowledged.

**Supporting Information Available:** Experimental details, EDX, XRD, SER and electrochemical data. This material is available free of charge via the Internet at <http://pubs.acs.org>.

LA703092C